Anti-control of Hopf bifurcation for the Willamowski–Rössler system

Liang Zhang[1] · **Qin Han**[2] · **Ziqiang Fang**[1] · **Songlin Peng**[1]

Abstract

Anti-control of Hopf bifurcation is one of the hot topics in nonlinear dynamics research, which is to make the system generate or strengthen bifurcation at a prespecified location. The Willamowski–Rössler system is taken as the research object, which is a nonlinear dynamic system derived from chemical reaction processes. Using the higher-dimensional Hopf bifurcation theory, the critical value of the Hopf bifurcation of a non-zero equilibrium point is obtained. A state feedback control method is proposed. With this method, anti-control of Hopf bifurcation for the system is accomplished by a hybrid controller, which is composed of linear and nonlinear controllers. The relationship between the bifurcation parameter and the control parameters of the linear controller is obtained. The values of the control parameters of the linear controller are determined by the bifurcation parameter. Although the critical values of the bifurcation parameters are not determined by the control parameters of the nonlinear controller, the parameter can change the amplitude of the limit cycle, which is inversely proportional to the amplitude of the limit cycle. Finally, the theoretical analysis is verified by numerical simulation.

Keywords Willamowski–Rössler system · Hopf bifurcation theory · Anti-control of Hopf bifurcation · State feedback control method

Mathematics Subject Classification 39A30 · 40A05 · 92D25 · 92C50

1 Introduction

Hopf bifurcation control and anti-control have become hotspots in nonlinear dynamics. The objective of Hopf bifurcation control is to delay the emergence of Hopf bifurcation by setting linear and nonlinear controllers, to expand the stable region of the system [1–5]. Anti-control of Hopf bifurcation is the inverse process of control. Setting the appropriate controller can make the Hopf bifurcation arise at the specified or expected position [6–11]. Cheng uses the Washout-filters method to achieve the anti-control of Hopf bifurcation for Chen's system by a delay feedback controller and analyzes the stability of the system [6]. By using explicit criteria, Yang carries out the anti-control of Hopf bifurcation for the three-dimensional Shimizu–Morioka system and analyzes the stability and bifurcation periodic solution of the system [7]. Chen sets up the appropriate controller for the system, which is to arise bifurcation at the expected position. Based on scour filter a dynamic anti-controller is proposed, in which the limit cycle of the system has oscillation behavior [8].

Liu studies the anti-control of the Hopf bifurcation for the four-dimensional Qi system with the linear and nonlinear controllers. By analyzing the characteristics of the Hopf bifurcation, the parameters of the linear and nonlinear controllers are determined [9]. Zhang analyzes the anti-control of the vibrating screen system by using a linear feedback controller. By adjusting the control parameters, the anti-control of Hopf–Hopf bifurcation can be realized, and the vibration mechanical efficiency can be improved [10]. Wen carries out the anti-control of Hopf bifurcation for centrifugal speed regulating system by using a feedback controller. The correctness of theoretical analysis is verified by simulation [11].

The Willamowski–Rössler system is one of the most common nonlinear reaction systems in chemistry. The system

✉ Liang Zhang
  lzhang08@163.com

  Qin Han
  hanqin08@163.com

1 School of Intelligent Manufacturing, Jianghan University, Wuhan 430056, People's Republic of China

2 College of Mechanical and Electrical Engineering, Wuhan Qingchuan University, Wuhan 430204, People's Republic of China

state variables represent the elements of chemical reactions. Each differential equation represents the rate of a chemical reaction. The system has obvious nonlinear characteristics. Bodale studies the chaos control of the Willamowski–Rössler system. Synchronous control is carried out by setting up a nonlinear controller for the system [12]. Aguda analyzes the synchronization characteristic and periodicity of the Willamowski–Rössler system and studies the oscillation characteristic of the system based on Shi'nikov theory [13]. Sun simulates the process of the Willamowski–Rössler system from period-doubling bifurcation to chaos state and then to period-doubling bifurcation again. The global exponential synchronization control of the system is realized by a controller [14]. Wu calculates the micromechanical system of the Willamowski–Rössler system and analyzes the dynamic characteristics of the noise of the system, as well as the interaction among the spatial degree of freedom, the size, and the internal fluctuation [15]. Chávez investigates the multi-step reaction mechanism of the Willamowski–Rössler system, which has oscillatory and chaotic dynamic characteristics. The condition of the appearance of bifurcation for the system is studied. The bifurcation which can lead to the arisen of simple or double chaotic characteristics—oscillatory attractor is verified [16]. Wang studies the chaos control of the Willamowski–Rössler system by using the continuous feedback control method and analyzes the influence of fluctuation on chaos control. The noise of the continuous feedback control method is instability [17]. Stucki analyzes the chaotic attractor and bifurcation of the Willamowski–Rössler system and studies the steady-state value and other nonlinear characteristics during oscillation [18]. At present, the researches mainly focus on the chaotic oscillation of the Willamowski–Rössler system and the analysis of chaos synchronization control of the system. The study of Hopf bifurcation is rare, especially the anti-control of Hopf bifurcation. By studying the anti-control of Hopf bifurcation for the Willamowski–Rössler system, the stable region of the system can be identified and expanded. Furthermore, stable chemical reaction rates can be obtained.

Based on the higher-dimensional Hopf bifurcation, the Hopf bifurcation characteristic of the Willamowski–Rössler system is analyzed in this paper. A state feedback control method is proposed to carry out the anti-control of Hopf bifurcation for the system. The Hopf bifurcation characteristics can arise at the specified position by changing the control parameters. The correctness of the theoretical analysis is verified by simulation.

The paper structure is arranged as follows: In Sect. 2, the differential equations of the Willamowski–Rössler system are introduced. In Sect. 3, the dynamical behavior of the system is investigated by Hopf bifurcation. In Sect. 4, a state feedback control method is proposed. In Sect. 5, with the state feedback control method, a hybrid controller is set up

for the system to anti-control of Hopf bifurcation. Finally, Sect. 6 summarizes this paper.

2 Willamowski–Rössler system

The Willamowski–Rössler system is proposed in reference [12]. It has the form:

$$\begin{cases} \dot{x}_1 = ax_1 - fx_1^2 - bx_1x_2 - dx_1x_3 \\ \dot{x}_2 = bx_1x_2 - cx_2 \\ \dot{x}_3 = -dx_1x_3 + ex_3 - gx_3^2 \end{cases} \tag{1}$$

where x_1, x_2, x_3 are state variables of the system, which represent the substances in a chemical reaction. a, b, c, d, e, f, g are positive real parameters, which represent the reaction speed. When the initial value is $(x_1, x_2, x_3)^T = (0.21, 0.01, 0.12)^T$ and the parameters are fixed as $[a, b, c, d, ef, g]^T = [30, 1, 10, 1, 16.5, 0.25, 0.5]^T$, the system has a chaotic attractor, which is shown in Fig. 1.

3 Hopf bifurcation

When $d^2 - fg \neq 0$, $b \neq 0$, $g \neq 0$, the system has six equilibrium points, given by:

$X_1 = (0, 0, 0)$, $X_2 = (\frac{a}{f}, 0, 0)$, $X_3 = (0, 0, \frac{e}{g})$, $X_4 = (\frac{c}{b}, \frac{ab-cf}{b^2}, 0)$, $X_5 = (\frac{de-ag}{d^2-fg}, 0, \frac{ad-ef}{d^2-fg})$,

$X_6 = \left(\frac{c}{b}, \frac{cd^2-bde+abg-cfg}{b^2g}, \frac{be-cd}{bg} \right)$.

Each equilibrium point has its own characteristics, which are equilibrium points with complex dynamic characteristics. Therefore, by analyzing the dynamic characteristics of anyone non-zero equilibrium point, we can understand the dynamic characteristics of the system. Taking the non-zero equilibrium point X_6 as the research object, the Hopf bifurcation characteristic of the system (1) is analyzed.

The Jacobi matrix of the system (1) at the equilibrium point X_6 is:

$$J(X_6) = \begin{bmatrix} -\frac{fc}{b} & -c & -\frac{dc}{b} \\ \frac{cd^2-bde+abg-cfg}{bg} & 0 & 0 \\ -\frac{bde-cd^2}{bg} & 0 & \frac{cd-be}{b} \end{bmatrix} \tag{2}$$

The characteristic equation of the system (1) is:

$$\lambda^3 + p_1\lambda^2 + p_2\lambda + p_3 = 0 \tag{3}$$

where $p_1 = \frac{cd}{b} + \frac{cf}{b} + e$, $p_2 = ac - \frac{c^2f}{b} - \frac{c^2df}{b^2} + \frac{cef}{b} + \frac{c^2d^2}{bg} + \frac{c^2d^3}{b^2g} - \frac{cde}{g} - \frac{cd^2e}{bg}$; $p_3 = ace - \frac{ac^2d}{b} + \frac{c^3df}{b^2} - \frac{c^2ef}{b} - \frac{c^3d^3}{b^2g} + \frac{2c^2d^2e}{bg} - \frac{cde^2}{g}$.

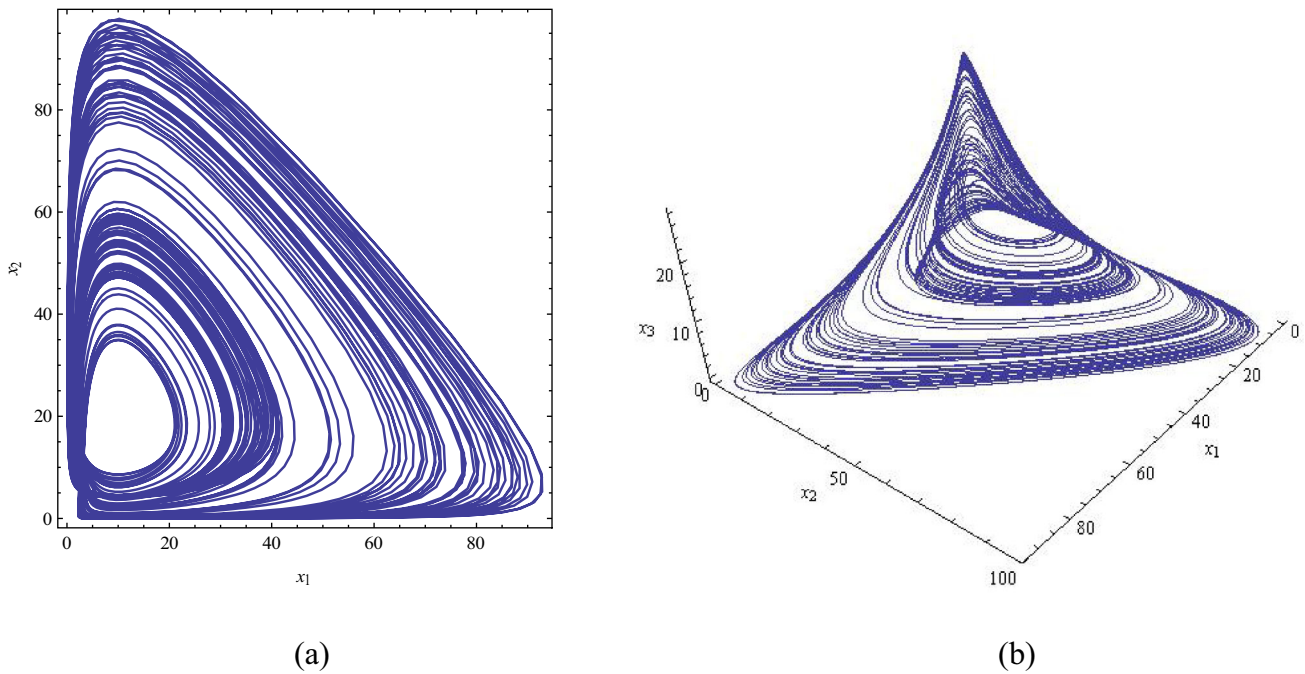(a)   (b)

Fig. 1 When $a = 30$, $b = 1$, $c = 10$, $d = 1$, $e = 16.5$, $f = 0.25$, $g = 0.5$, the chaotic attractor of the system (1)

Based on the Routh–Hurwitz criterion, the conditions for the existence of Hopf bifurcation at the equilibrium point X_6 are as follows:

$$p_1 > 0, \ p_2 > 0, \ p_1 p_2 - p_3 = 0$$

Taking the real parameter e as the bifurcation parameter of the system (1), the critical value of Hopf bifurcation can be obtained as follows:

$$e_0 = \frac{cQ_1 + \sqrt{cf Q_2}}{2b(d^2 - fg)}$$

where

$Q_1 = 2d^3 - d^2 f + f^2 g - df(b + 2g)$,
$Q_2 = (d^2 - fg)[2bcf(d - 2g) + cf(d^2 - fg) + 4ab^2 g] + b^2 cd^2 f$.

When $e = e_0$, the characteristic Eq. (2) of the system has a pair of pure imaginary roots $\lambda_{1,2} = \pm i\omega_0 = \pm i\sqrt{Q_3 + Q_4 e_0}$, and a negative real root $\lambda_3 = -(\frac{cd}{b} + \frac{cf}{b} + e_0)$. where $Q_3 = \frac{c}{b^2 g}[ab^2 g + c(d^2 - fg)(b + d)]$, $Q_4 = \frac{cf}{b} - \frac{cd}{g} - \frac{cd^2}{bg}$.

From the characteristic Eq. (3), we get

$$\lambda'(e) = -\frac{\lambda^2 + Q_4\lambda + Q_5 - \frac{2cd}{g}e}{3\lambda^2 + 2\left(\frac{cd}{b} + \frac{cf}{b} + e\right)\lambda + Q_3 + Q_4 e} \quad (4)$$

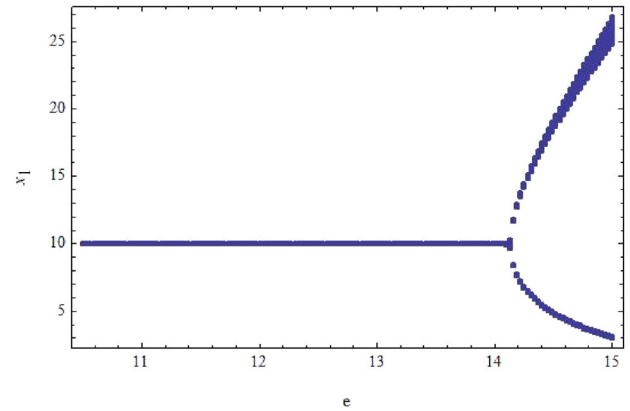where $Q_5 = ac - \frac{c^2 f}{b} + \frac{2c^2 d^2}{bg}$.

Fig. 2 When $a = 30$, $b = 1$, $c = 10$, $d = 1$, $f = 0.25$, $g = 0.5$, the bifurcation diagram of the system (1)

Substituting the value of pure imaginary root $+i\omega_0$ and e_0 into the Eq. (4).

$$\mathrm{Re}(\lambda'(e)) = \frac{2(Q_3 + Q_4)}{gT}\left[2cde_0 + gQ_3 \right.$$
$$\left. + gQ_4(2e_0 + \frac{cd + cf}{b}) - gQ_5\right] \neq 0 \quad (5)$$

$$\mathrm{Im}(\lambda'(e)) = -\frac{2\sqrt{Q_3 + e_0 Q_4}}{gT}[gQ_4(Q_3 + e_0 Q_4)$$
$$- \left(\frac{cd + cf}{b} + e_0\right)(2cde_0 + gQ_3 + e_0 gQ_4$$
$$- -gQ_5)] \neq 0 \quad (6)$$

where $T = 4(Q_3 + Q_4 e_0)\left[\left(\frac{cd+cf}{b} + e_0\right)^2 + Q_3 + Q_4 e_0\right]$.

The transversality is satisfied. According to the higher-dimensional Hopf bifurcation theory, when $e = e_0$, the Hopf bifurcation of the system is appeared.

When $a = 30, b = 1, c = 10, d = 1, f = 0.25, g = 0.5$, the critical value of Hopf bifurcation is $e_0 = 14.137$ and the Hopf bifurcation of the system is appeared. The bifurcation diagram of the system is shown in Fig. 2.

When $e = 13.5$, the equilibrium point X_6 is gradually stable, as shown in Fig. 3.

When $e = 15$, the equilibrium point X_6 is unstable and the system has a stable periodic solution, as shown in Fig. 4.

4 State feedback control method

According to the high-dimensional Hopf bifurcation theory, the n-dimensional dynamic system is defined as:

$$\dot{x} = f(x, \mu) \tag{7}$$

where $f : R^{n+1} \to R^n$, $x \in R^n$, $\mu \in R$. x is the system state variable. μ is the real parameter of the system. f is continuously differentiable for x and μ in the domain.

Suppose the equilibrium point of the system (7) is $X^e = \left(X_1^e, X_2^e, \cdots, X_i^e, \cdots, X_n^e\right)$, $i \geq 1$. The Jacobian matrix of the system at X^e is $J(X^e, \mu)$. If the conditions are satisfied [19]:

(1) Jacobian matrix $J(X^e, \mu^e)$ has a pair of pure imaginary root eigenvalues $\lambda(\mu^e) = \pm i\omega$, other eigenvalues have negative real parts;
(2) When the eigenvalue $\lambda(\mu^e)$ is nonzero, it crosses the imaginary axis.

$$\left. \frac{d(Re\lambda(\mu))}{d\mu} \right|_{\mu=\mu^e} \neq 0$$

The Hopf bifurcation of the system appears at μ^e.

For the anti-control of Hopf bifurcation, the controller should be set up to the system. Defined

$$\begin{cases} u = u(x, y) \\ \dot{y} = h(x, y) \end{cases} \tag{8}$$

where $y \in R^m (1 \leq m \leq n)$ is the new state variable of the system. The controller $u(x, y)$ and range $h(x, y)$ are continuously differentiable for x and y. The controller is a hybrid controller, which is composed of linear and nonlinear controllers. Namely

$$\begin{cases} u_j(x_j, y_j) = k_{1j}x_j + k_{2j}(x_j - X_i^e)^3 - k_{3j}y_j \\ \dot{y} = u_j(x_j, y_j) \end{cases} \tag{9}$$

where X_i^e is the state variable at any equilibrium point of the system (7). The parameters of the controller are: $k_{1j} = (k_{11}, k_{12}, \cdots, k_{1m})$, $k_{2j} = (k_{21}, k_{22}, \cdots, k_{2m})$, $k_{3j} = (k_{31}, k_{32}, \cdots, k_{3m})$.

Then the controlled system is

$$\begin{cases} \dot{x} = f(x, y) + u(x, y) \\ \dot{y} = h(x, y) \end{cases} \tag{10}$$

where $u(x, y) = (u_1(x_1, y_1), \cdots u_m(x_m, y_m), 0, \cdots, 0)_n^T$, $h(x, y) = (u_1(x_1, y_1), \cdots u_m(x_m, y_m))^T$.

According to Laplace transform, suppose $z_j = k_{1j}x_j + k_{2j}(x_j - X^e)^3$ as a function of x_j. It is substituted into the second Eq. (9). The results are as follows:

$$u_j(s) = z_j(s) - k_{3j}y_j(s) \tag{11}$$

$$z_j(s) = (s + k_{3j})y_j(s) \tag{12}$$

Define

$$G_j(s) = \frac{u_j(s)}{z_j(s)} = \frac{s}{s + k_{3j}} \tag{13}$$

Therefore, k_{3j} is a positive real number.
The controlled system is defined as:

$$\dot{X} = F(X, \mu) \tag{14}$$

where $\dot{X} = (x, y)^T$, $F = (f(x, y) + u(x, y), h(x, y))^T$.

Suppose $J_C(X, \mu) = \frac{\partial F(X, \mu)}{\partial X}$ is the Jacobi matrix of the controlled system (14).

$$J_C(X, \mu) = \begin{bmatrix} J(x) + P_1(x) & P_2(x) \\ P_3(x) & P_4(x) \end{bmatrix}$$

where $J(x)$ is the Jacobi matrix of the original system. Namely

$$J(x) = \frac{\partial f(x, \mu)}{\partial x}, \quad P_1(x) = \frac{\partial u(x, y)}{\partial x}, \quad P_2(x) = \frac{\partial u(x, y)}{\partial y},$$
$$P_3(x) = \frac{\partial h(x, y)}{\partial x}, \quad P_4(x) = \frac{\partial h(x, y)}{\partial y}.$$

We define as $P_1(x) = \begin{bmatrix} M & 0_{(n-m)\times(n-m)} \\ 0_{(n-m)\times(n-m)} & 0_{(n-m)\times(n-m)} \end{bmatrix}$,

$$P_2(x) = \begin{bmatrix} N \\ 0_{(n-m)\times(n-m)} \end{bmatrix}, \quad P_3(x) = \begin{bmatrix} M & 0_{(n-m)\times(n-m)} \end{bmatrix},$$
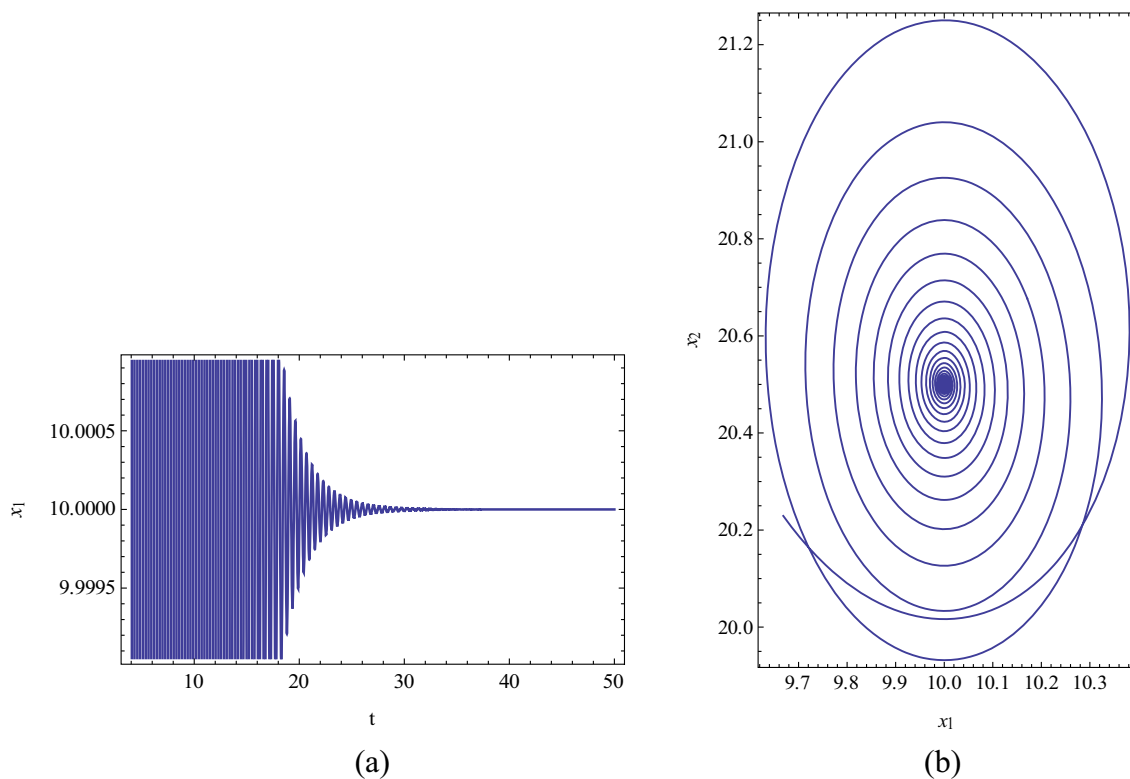
Fig. 3 When $a = 30$, $b = 1$, $c = 10$, $d = 1$, $f = 0.25$, $g = 0.5$ and $e = 13.5$, sequence diagram and phase diagram of the system (1)
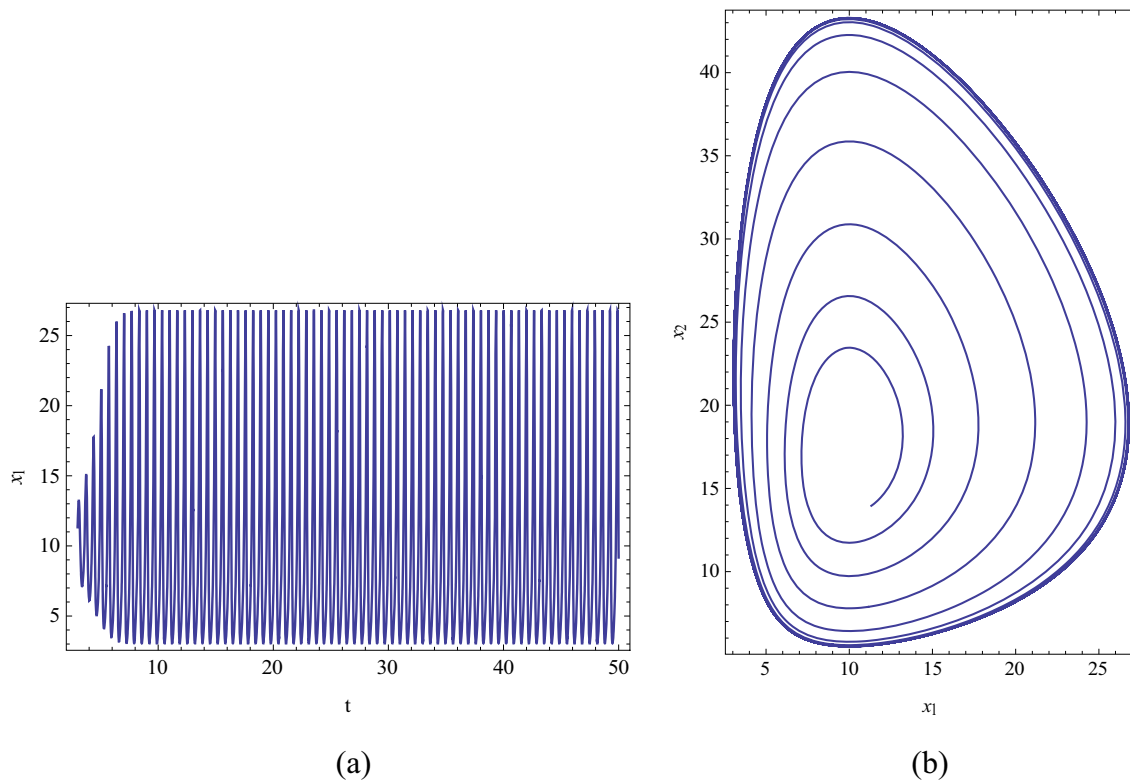

Fig. 4 When $a = 30$, $b = 1$, $c = 10$, $d = 1$, $f = 0.25$, $g = 0.5$ and $e = 15$, sequence diagram and phase diagram of the system (1)

$P_4(x) = N$.where

M

$$= \begin{bmatrix} k_{11} + 3k_{21}(x_1 - X_1^e)^2 & \cdots & 0 \\ \vdots & \ddots & \vdots \\ 0 & \cdots & k_{1m} + 3k_{2m}(x_m - X_m^e)^2 \end{bmatrix},$$

$$N = \begin{bmatrix} k_{31} & \cdots & 0 \\ \vdots & \ddots & \vdots \\ 0 & \cdots & k_{3m} \end{bmatrix}$$

The characteristic equation of the Jacobi matrix $J_C(X, \mu)$ of the controlled system (14) at the equilibrium point X^e is obtained as follows:

$$Q(\lambda, \mu_e) = q_0(\mu_e)\lambda^{n+m} + q_1(\mu_e)\lambda^{n+m-1} + \cdots + q_{n+m}(\mu_e) \tag{15}$$

Suppose

$$H_n = \begin{bmatrix} q_1(\mu_e) & q_0(\mu_e) & \cdots & 0 \\ q_3(\mu_e) & q_2(\mu_e) & \cdots & 0 \\ \vdots & \vdots & \ddots & \vdots \\ q_{2(n+m)-1}(\mu_e) & q_{2(n+m)-2}(\mu_e) & \cdots & q_{n+m}(\mu_e) \end{bmatrix}$$

When the following conditions are met:

$$\begin{cases} q_{n+m}(\mu_e) > 0 \\ \Delta_\omega(\mu_e) = \det[H_i(\mu_e)] > 0, \ \omega = 1, 2, \cdots, n+m-2 \\ \left. \frac{d(\Delta_{n+m-1}(\mu))}{d\mu} \right|_{\mu=\mu_e} \neq 0 \end{cases}$$

The Hopf bifurcation of the controlled system (14) is occurred. According to

$$\Delta_{n+m-1}(\mu_e) = \det\left[H_{n+m-1}(\mu_e)\right] = 0$$

the control parameters of the controlled system (14) are determined.

5 Anti-control of Hopf bifurcation

According to the state feedback control method, a controller $u_1(x_1, y_1)$ is set for the system (1). The controlled system is as follows:

$$\begin{cases} \dot{x}_1 = ax_1 - fx_1^2 - bx_1x_2 - dx_1x_3 \\ \dot{x}_2 = bx_1x_2 - cx_2 + k_{11}x_1 + k_{21}(x_1 - X_{11}^e)^3 - k_{31}y \\ \dot{x}_3 = -dx_1x_3 + ex_3 - gx_3^2 \\ \dot{y} = k_{11}x_1 + k_{21}(x_1 - X_{11}^e)^3 - k_{31}y \end{cases} \tag{16}$$

Equilibrium point $X_6' = (X_1, X_2, X_3, Y_4)$ of the controlled system (16) is

$$X_{6'} = \left(\frac{c}{b}, \frac{cd^2 - bde + abg - cfg}{b^2 g}, \frac{be - cd}{bg}, \frac{b^2 ck_{11} + (c - bX_{11}^e)^3 k_{21}}{b^3 k_{31}} \right)$$

According to the state feedback control method, each matrix is as follows:

$$J(X_6') = \begin{bmatrix} -\frac{fc}{b} & -c & -\frac{dc}{b} \\ \frac{cd^2 - bde + abg - cfg}{bg} & 0 & 0 \\ -\frac{bde - cd^2}{bg} & 0 & \frac{cd - be}{b} \end{bmatrix}, \ P_1(x)$$

$$= \begin{bmatrix} 0 & 0 & 0 \\ k_{11} & 0 & 0 \\ 0 & 0 & 0 \end{bmatrix}, \ P_2(x) = \begin{bmatrix} 0 \\ -k_{31} \\ 0 \end{bmatrix}$$

$$P_3(x) = \begin{bmatrix} M & 0 & 0 & 0 \end{bmatrix}, P_4(x) = N.$$

The Jacobi matrix of the controlled system (16) at the equilibrium point X_6' is:

$$J_c(X_6') = \begin{bmatrix} -\frac{fc}{b} & -c & -\frac{dc}{b} & 0 \\ \frac{cd^2 - bde + abg - cfg}{bg} + k_{11} & 0 & 0 & -k_{31} \\ -\frac{bde - cd^2}{bg} & 0 & \frac{cd - be}{b} & 0 \\ k_{11} & 0 & 0 & -k_{31} \end{bmatrix}$$

The characteristic equation of the Jacobi matrix $J_c(X_6')$ is written as

$$Q(\lambda, \mu_e) = q_0(\mu_e)\lambda^4 + q_1(\mu_e)\lambda^3 + q_2(\mu_e)\lambda^2 + q_3(\mu_e)\lambda + q_4(\mu_e) \tag{17}$$

where $q_0(\mu_e) = 1, q_1(\mu_e) = k_{31} + e + \frac{c}{b}(f - d)$,

$$q_2(\mu_e) = \frac{1}{b^2 g}\left(bc^2d^2 + c^2d^3 - b^2cde - bcd^2e + ab^2cg \right.$$
$$\left. - bc^2fg - c^2dfg + bcefg + b^2gck_{11} \right.$$
$$\left. - bcgdk_{31} + b^2gek_{31} + bcfgk_{31} \right)$$

$$q_3(\mu_e) = \frac{1}{b^2 g}\left[ab^2gck_{31} - c\left(c^2d^3 - 2bcd^2e \right.\right.$$
$$+ b^2de^2 + abcdg - ab^2eg - c^2dfg$$
$$+ bcgdk_{11} - b^2gek_{11} + b^2dek_{31} + bcgfk_{32}$$
$$\left.\left. + cdgfk_{31} - begfk_{31} - bcd^2k_{31} - cd^3k_{31} + bd^2ek_{31} \right)\right],$$

$$q_4(\mu_e) = \frac{ck_{31}(be - cd)(bde - cd^2 - abg + cfg)}{b^2 g}.$$

When $a = 30$, $b = 1$, $c = 10$, $d = 1$, $f = 0.25$, $g = 0.5$, the relationship between the bifurcation parameter e and the control parameters k_{11}, k_{31} is obtained.
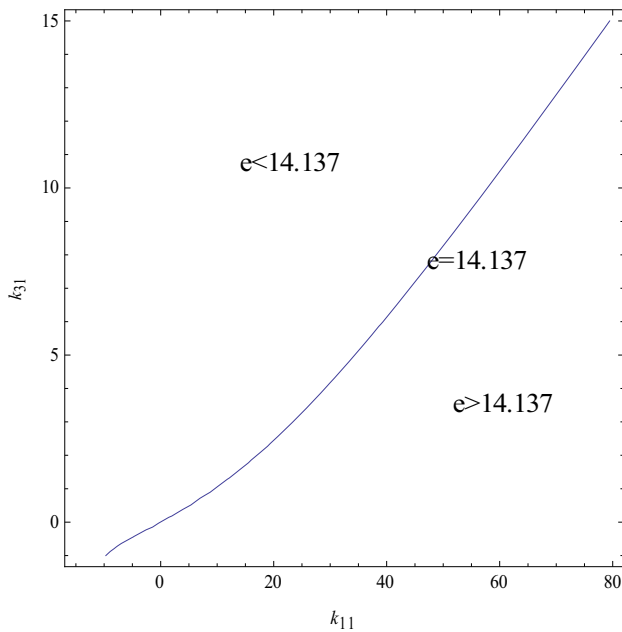
Fig. 5 Range of bifurcation parameter e

Fig. 6 When $k_{11} = 68.823, k_{31} = 0.5$, the bifurcation diagram of controlled system (16)
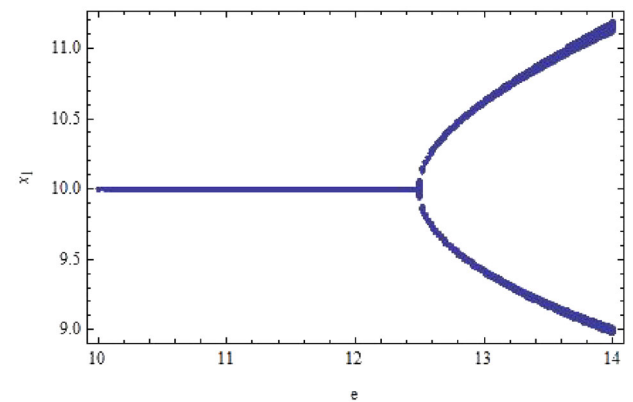
Fig. 7 When $k_{11} = -5.13, k_{31} = 0.5$, the bifurcation diagram of controlled system (16)

$$350(e - 23.75)(e - 14.1375)(e - 10)(e - 0.505)$$
$$+\left(1.235 \times 10^6 - 80187.5e - 10859.4e^2 + 656.25e^3\right)k_{31} - 17.5$$
$$\times (e + 29.401)\left(e^2 - 36.115e + 368.792\right)k_{31}^2$$
$$-17.5(e - 10.034)(e + 10.82)k_{31}^3 + k_{11}^2$$
$$[250e + (100e - 1000)k_{31} - 2500]$$
$$+[-175(e - 10) \times (e - 15.66)(e + 3.876)$$
$$+10k_{31}(e - 10.148)(e - 29.25)(e - 5.6)$$
$$+10k_{31}^2(e - 44.856)(e - 10.14)]k_{11} = 0$$

By determining the value of the bifurcation parameter e which Hopf bifurcation occurs at the expected point, the values of the control parameters k_{11} and k_{31} can be determined. When the bifurcation parameter $e < 14.137$, the Hopf bifurcation of the system appears ahead of time and the stable region decreases. When the bifurcation parameter $e > 14.137$, the Hopf bifurcation of the system is delayed, which expands the stable region. The object of anti-control of the Hopf bifurcation for the Willamowski–Rössler system is realized. The relationship between the value range of the bifurcation parameter e and the control parameters k_{11} and k_{31} is shown in Fig. 5.

When the bifurcation parameter $e = 20$ and the control parameter $k_{31} = 0.5$, the other control parameter is $k_{11} = 68.823$. The bifurcation diagram of the system is shown in Fig. 6.

When the bifurcation parameter $e = 12.5$ and the control parameter $k_{31} = 0.5$, the other control parameter is
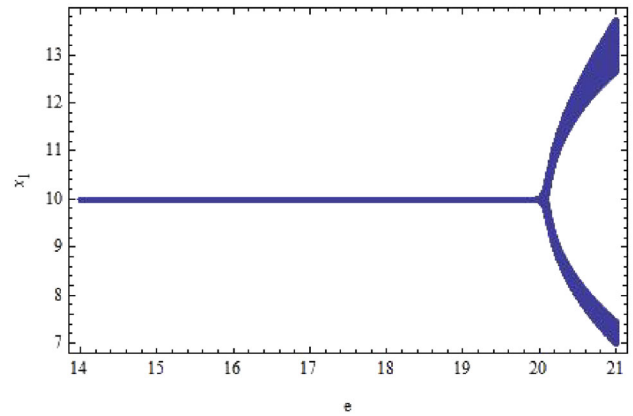
$k_{11} = -5.13$. The bifurcation diagram of the system is shown in Fig. 7.

Although the control parameter k_{21} can not change the bifurcation parameter e, the amplitude of the limit cycle for the system can be altered by it, as shown in Fig. 8.

From the above analysis, it shows that the control parameter k_{21} has no effect on the value of the bifurcation parameter e, but the control parameter k_{21} has an effect on the amplitude of the bifurcation limit cycle. With increasing the value of k_{21}, the amplitude of the limit cycle gradually decreases, which the anti-control of the amplitude of the limit cycle can be realized.

6 Conclusion

In this paper, we have considered the anti-control of Hopf bifurcation for the Willamowski-Rössler system. According to the high dimensional Hopf bifurcation theory, the characteristics of Hopf bifurcation at the non-zero equilibrium point
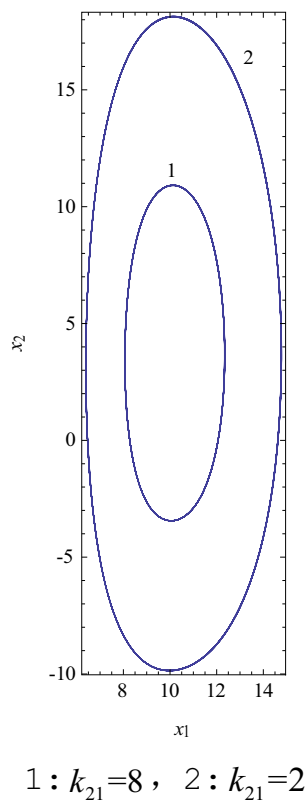
$$1 : k_{21}=8 \ , \ \ 2 : k_{21}=2$$

Fig. 8 Amplitude of limit cycle of controlled system (16) is influenced by different k_{21}

of the system are analyzed, and the critical value of Hopf bifurcation is studied. When $a = 30, b = 1, c = 10, d = 1,$ $f = 0.25, g = 0.5$, the critical value of the Hopf bifurcation parameter e of the system is $e_0 = 14.137$. Therefore, when $e < e_0$, the system is gradually stable. When $e > e_0$, the system is unstable.

A state feedback control method is proposed. Anti-control of Hopf bifurcation for the Willamowski- Rössler system is carried out by setting a hybrid controller, which is composed of linear and nonlinear controllers. The relationship between the control parameters and the bifurcation parameter is obtained. By specifying the position of Hopf bifurcation, the values of the control parameters are determined, and the purpose of anti-control is realized. Namely, the advance or delay of Hopf bifurcation is determined by the control parameters of the linear controllers, and the amplitude of the limit cycle is determined by the control parameter of the nonlinear controller. The correctness of the theoretical analysis is verified by numerical simulation.

Author contribution Liang Zhang is mainly responsible for analyzing and writing. Qin Han is responsible for partial simulation analysis. Ziqiang Fang is responsible for partial simulation analysis. Songlin Peng is responsibal for revising this paper.

Data availability Not applicable.

Competing interests I declar that there is no competition.

References

1. Zhang L, Tang JS, Han Q (2018) Hopf bifurcation control of a Pan-Like chaotic system. Chin Phys B 27(9):094702
2. Zhu LH, Zhao HY, Wang XM (2015) Bifurcation analysis of a delay reaction–diffusion malware propagation model with feedback control. Commun Nonlinear Sci Numer Simul 22(1):747–768
3. Xu Y, Ma SJ, Zhang HQ (2011) Hopf bifurcation control for stochastic dynamical system with nonlinear random feedback method. Nonlinear Dyn 65(1):77–84
4. Ding DW, Wang C, Ding LH et al (2016) Hopf bifurcation control in a FAST TCP and RED model via multiple control schemes. J Control Sci Eng 2016(4):1–10
5. Ding YT, Jiang WH, Wang HB (2010) Delayed feedback control and bifurcation analysis of Rossler chaotic system. Nonlinear Dyn 61(4):707–715
6. Cheng ZS (2010) Anti-control of Hopf bifurcation for Chen's system through washout filters. Neurocomputing 73(16):3139–3146
7. Yang Y, Liao XF, Dong T (2017) Anti-control of Hopf bifurcation in the Shimizu-Morioka system using an explicit criterion. Nonlinear Dyn 89(1):1453–1461
8. Chen DS, Wang HO, Chen GR (2001) Anti-control of Hopf bifurcations. IEEE Trans Circuits Syst IFTA 48(6):661–672
9. Liu SH, Tang JS (2008) Anti-control of Hopf bifurcation at zero equilibrium of 4D Qi system. Acta Phys Sin 57(10):6162–6167
10. Zhang SJ, Du WX, Yin S (2017) Anti-control of Double Hopf bifurcation of vibration rating griddle system. J Hunan Univ (Nat Sci) 44(10):55–61
11. Wen GL, Xu HD, Lv ZY et al (2015) Anti-controlling Hopf bifurcation in a type of centrifugal governor system. Nonlinear Dyn 81(1):811–822
12. Bodalea ILIE (2015) VICTOR Andrei Oancea. Chaos control for Willamowski–Rössler model of chemical reactions. Chaos Solitons Fractals 78:1–9
13. Aguda BD, Clarke BL (1988) Dynamic elements of chaos in the Wiliamowski–Rössler network. J Chem Phys 89:7428
14. Sun WP, Wang HY, Kan M (2018) Numerical simulation, control and synchronization research on chaotic behavior of Wiliamowski–Rössler System. J Dyn Control 16(1):35–40
15. Wu XG, Raymond K (1993) Internal fluctuations and deterministic chemical chaos. Phys Rev Lett 70(13):1940–1943
16. Chávez F, Kapral R (2002) Oscillatory and chaotic dynamics in compartmalized geometries. Phys Rev 65:056203

17. Wang HL, Xin HW (1995) Control of chemical chaos and influence of fluctuations. Chin J Chem Phys 8(2):129–132

18. Stucki JW, Urbanczik R (2005) Entropy production of the Willamowski–Rössler Oscillator. Zeitschrift Für Naturforschung A 60a:599–607

19. Nguyen LH, Hong KS (2012) Hopf bifurcation control via a dynamic state-feedback control. Phys Lett A 376:442–446